

JUPITER'S RADIATION BELTS AND UPPER ATMOSPHERE

JOSEPH J. DEGIOANNI and JOHN R. DICKEL

University of Illinois Observatory, Urbana, Ill., U.S.A.

Abstract. Models of Jupiter's radiation belts have been constructed to determine the distribution of particles and their energies which will produce the observed decimetric radio emission. Data on the spectrum and the variation of emission with Jovian longitude have been used to show that the relativistic particles have a nearly isotropic distribution with high energies (of order 100 MeV) within 2 Jovian radii and a very flat distribution in the equatorial plane of low energy particles further out in the magnetosphere.

Subtraction of the emission predicted by this model from the total radio emission shows that the thermal contribution in the frequency range between 3000 and 10000 MHz is somewhat less than had been previously expected. (The brightness temperature of the planetary disk is 180K at 3000 MHz, for example.) This suggests that the ammonia mixing ratio in Jupiter's upper atmosphere may be as high as 0.002.

1. Introduction

The microwave radio emission of Jupiter is composed of 2 parts as seen in Figure 1: non-thermal emission from Jupiter's radiation belts and thermal emission from the upper atmosphere. Detailed study of this emission can therefore be used to improve our knowledge of both regions of the Jovian environment. To this end we have constructed theoretical models of the radiation belts and compared these with the observational data to obtain the physical parameters of the belts. These results are then also used to improve the models of the thermal emission from the atmosphere.

2. The Radiation Belts of Jupiter

2.1. CONSTRUCTION OF THE MODEL

In our simplified model, the Jovian radiation belts are assumed to consist of relativistic electrons, whose motions can be described by the guiding center approximation, trapped in a dipolar magnetic field inclined ten degrees to the axis of the rotation of the planet. Synchrotron emission from these electrons results in the observed non-thermal microwave spectrum. The IBM 360/75 computer at the University of Illinois was used to calculate the Stokes parameters of the synchrotron radiation integrated over a given dipolar shell as a function of the surface magnetic field and the electron energy. The integration takes into account the partial eclipse of the dipolar shells by the planet at different System III longitudes. In addition, the Stokes parameters are integrated separately for two types of electron populations, i.e. one whose pitch angle distribution is isotropic and another whose distribution is sharply confined to the magnetic equator.

2.2. FITTING TO THE OBSERVATIONAL PROPERTIES

2.2.1. *Intensity Profiles*

The magnetosphere is divided into two zones near the approximate distance at which

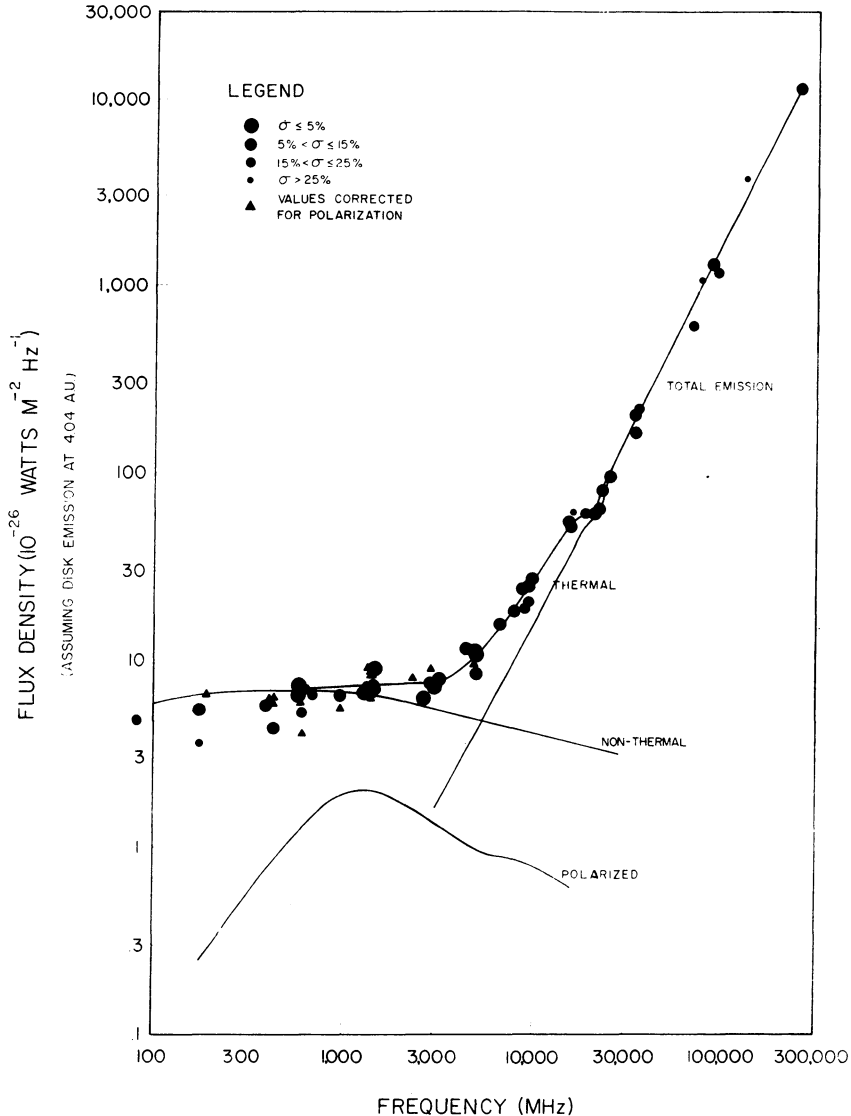


Fig. 1. The radio spectrum of Jupiter.

the gravitational and the centrifugal forces are equal and oppose each other; this happens at $L=2$ where L is the equatorial distance from the center of the planet in Jovian radii. The intensity of the emission as a function of shell distance for $L > 2$ was approximated by a decreasing function of distance from the planet as best fits the observational results of Branson (1968) and Gulkis (1970) at 21 cm. The inner zone ($1 < L < 2$) is described by more rapidly varying function whose position of peak intensity is a model parameter which was adjusted to best fit the polarization observations (see Section 3 below). Figure 2 shows how the extent of the emission varies with

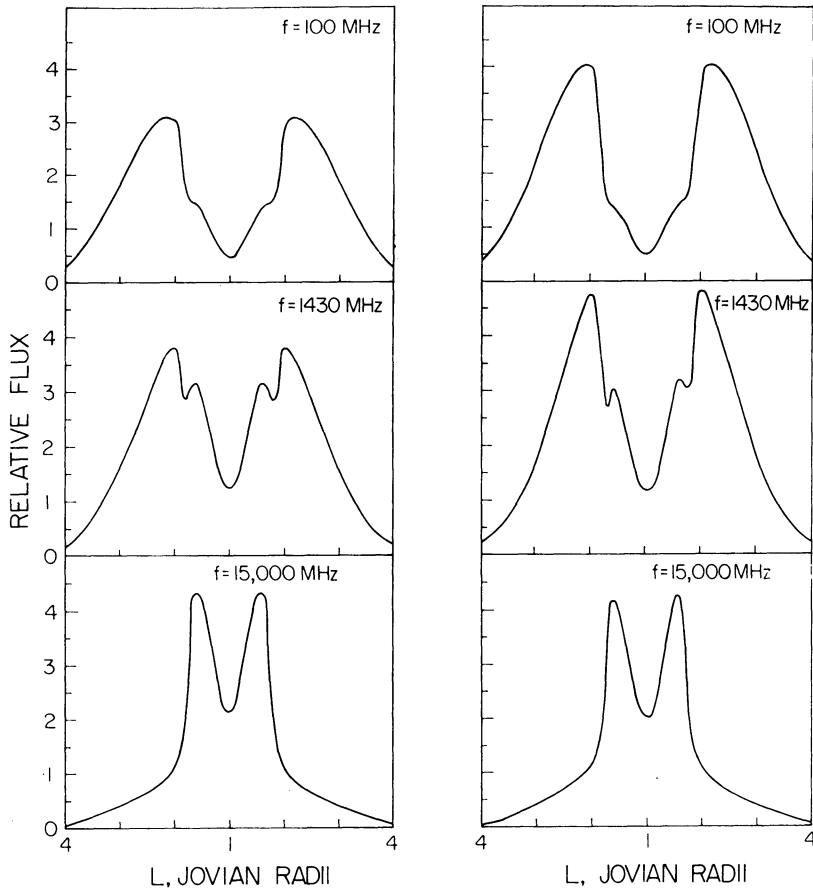


Fig. 2. The intensity profiles at $\lambda_{III} = 198^\circ$ and $\lambda_{III} = 288^\circ$.

frequency. In agreement with the observations by Gulkis (1970), the emission at higher frequencies is mainly produced in the region $1 < L < 2$ (the inner zone), whereas at lower frequencies much of the emission is produced in the outer zone ($L > 2$). The profiles to the left (Figure 2) correspond to System III longitude of 198° and to the right for a longitude of 288° . The latter shows a certain degree of east-west asymmetry caused by the partial eclipse of the planet. This effect has also been observed by Branson (1968).

2.2.2. Variation of Intensity of Emission with Rotation

The variations in intensity of emission with rotation of the planet are mainly determined by the outer zone where a major portion of the particles are confined to the magnetic equator. This effect, of course, is a direct consequence of the sharp beaming of synchrotron emission in the plane of oscillation of the relativistic electrons. The amplitude of the variations is a very sensitive function of the degree of confinement as

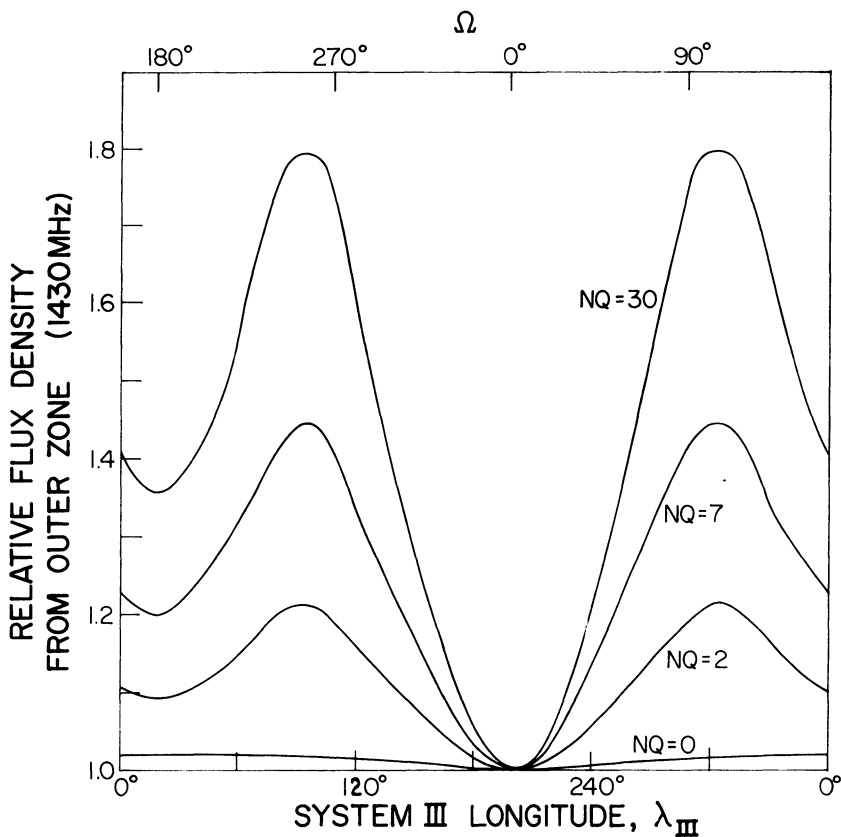


Fig. 3. Variation of flux density at 1430 MHz (outer zone) as a function of NQ .

shown in Figure 3 where NQ is a measure of the fraction of particles whose motion is limited to the plane of the magnetic equator. Figure 4 shows how the predicted variations compare with the observations at 2600 MHz and 600 MHz by Roberts and Ekers (1968). The oscillations at 2600 MHz contain a nonvariable contribution of 20% from the thermal component.

2.2.3. Spectrum of the Degree of Polarization

The fractional degree of polarization is a very sensitive function of the equatorial pitch angle distribution of the particles. Thus, we find that the pitch angle distribution in the inner zone, where most of the emission at high frequencies is produced, must be isotropic if we hope to fit the observed polarization spectrum. In addition, for an isotropic distribution of particles, the degree of polarization is a rapidly varying function of the location within the inner zone, as shown in Figure 5. This fact imposes an important constraint as to the location and shape of the intensity profile from the inner zone. The predicted polarization spectrum is shown in Figure 6. In particular, the rapid decline of the degree of polarization at higher frequencies is in good agree-

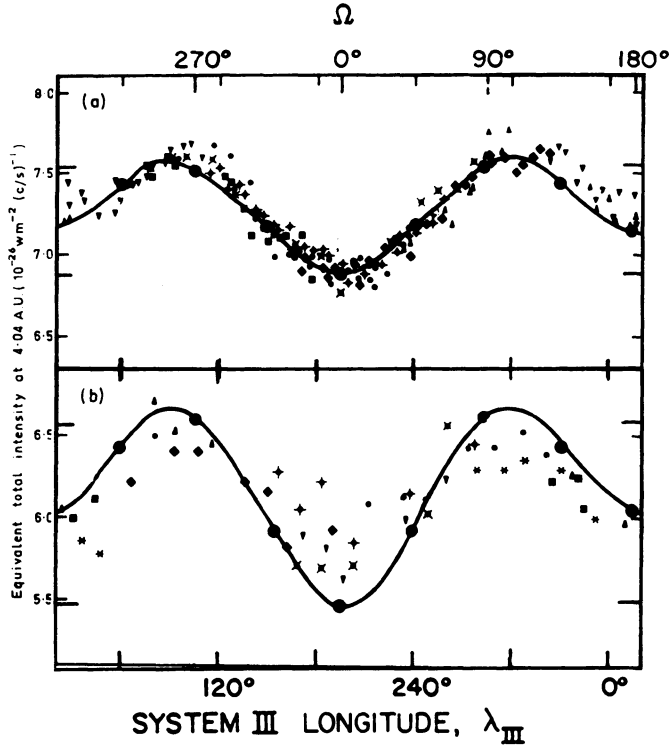


Fig. 4. Variations of flux density at 2600 MHz (upper curve) and 600 MHz (lower curve) as compared with the observations by Roberts and Ekers (1968).

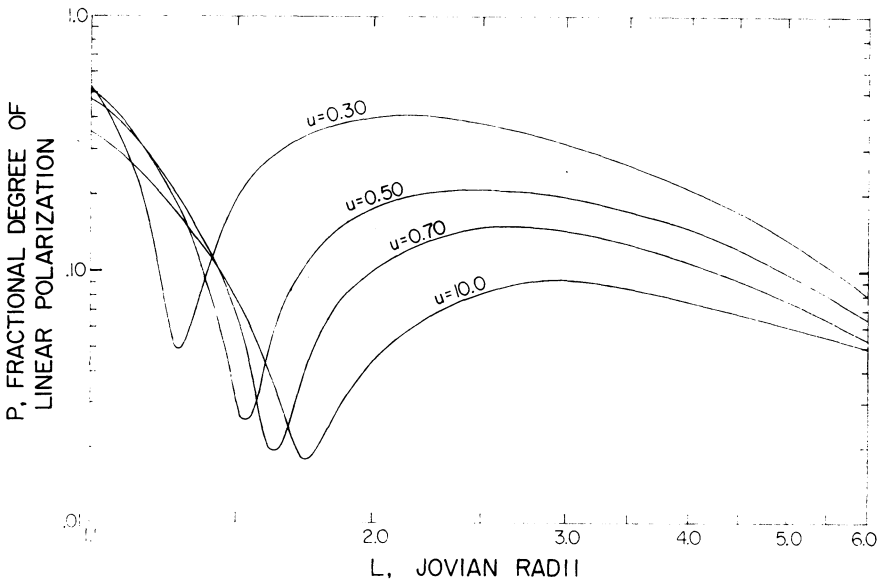


Fig. 5. Fractional degree of polarization as a function of L and u (u is an energy-dependent variable).

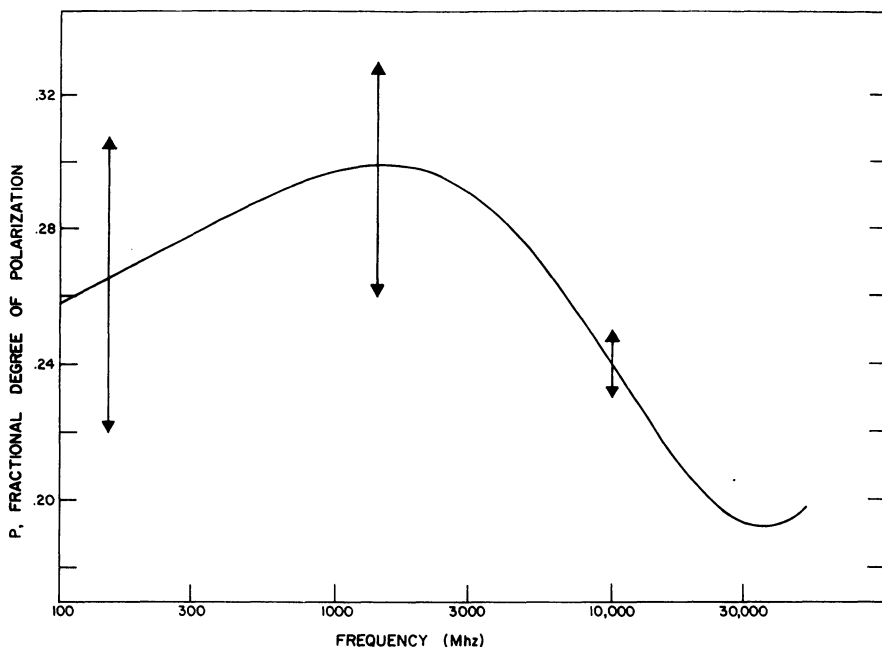


Fig. 6. Spectrum of the degree of polarization.

ment with the observations (Dickel *et al.*, 1970). The arrows in Figure 6 show the range of variation in the degree of polarization with the rotation of the planet.

2.2.4. Spectrum of the Non-Thermal Emission

The shape of the non-thermal spectrum is determined by the energy distribution of the electrons in the outer and inner zones. We find that two distinct energy distributions, rather than a gradient of energy across the dipolar shells, give the best agreement with the observational results (Dickel *et al.*, 1970). Our best model, included in Figure 1, predicts a relatively flat non-thermal spectrum. As a consequence, the thermal contribution to the total emission at higher frequencies (> 3000 MHz) appears to be less than previously anticipated. This result will be elaborated upon in Section 3.

2.3. SUMMARY OF CHARACTERISTICS OF JUPITER'S RADIATION BELTS

The properties of the radiation belts are shown in Table I. The inner zone has a relatively uniform electron density population with a peak intensity of the emission near 1.6 Jovian radii. The electron densities refer to equatorial values and, of course, show a rapid decline with magnetic latitude especially in the outer zone. The equatorial density in the outer zone falls approximately as L^{-4} which is similar to the distribution of the thermal plasma in that region as derived in a model of the plasmasphere by Melrose (1967). The equatorial pitch angle distribution is nearly isotropic for the inner zone ($1 < L < 2$) and becomes 80% confined to a flat equatorial distribution for

TABLE I
Parameters of Jupiter's radiation belts

	Inner zone	Outer zone
Equatorial distance from center of Jupiter	1.6 R	$> 2.0 R$
Peak relativistic ^a electron density	1 cm^{-3}	2 cm^{-3}
Equatorial density distribution	uniform	$\sim (R/R)^{-4}$
Mean electron energy ^a	18 MeV	6 MeV
Pitch angle distribution	isotropic	80% of particles confined to equator (with distribution of $\sin^{60} \alpha$)

^a Values assume B_{surface} of 30 G.

$L > 2$ (i.e., with pitch angles which follow a distribution of the form $\sin^{60} \alpha$). The electron densities and estimated mean electron energies are obtained if we assume a surface magnetic field of 30 G. A plot of the electron flux as function of latitude and planetary distance is shown in Figure 7. There is little fine structure except near $L=2$ where

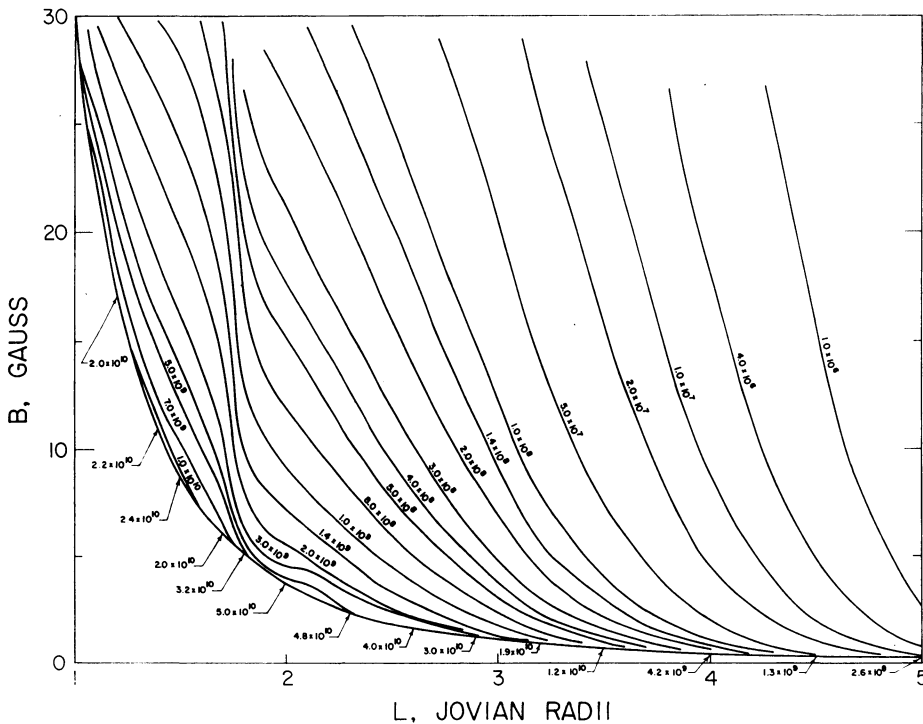


Fig. 7. B - L plot of the electron flux for a surface, equatorial magnetic field of 30 G.

the two zones merge with each other. These values are of the order of 1000 times those which have been observed in the radiation belts of the Earth.

3. Implications of the Non-Thermal Spectrum upon the Jovian Upper Atmosphere

The current more detailed model of the Jovian radiation belts predicts a relatively flat non-thermal spectrum out to fairly high frequencies (3000 MHz to 15000 MHz). Thus, it appears that the thermal contribution to the total emission is less than previously anticipated from the models of Berge (1966) and Branson (1968). In particular, the thermal component at 3000 MHz is reduced to a temperature of approximately 180 K. Figure 8 shows the Jovian thermal spectrum compared with the observational results.

The current model gives a strong indication for the flattening of the Jovian thermal spectrum out to at least 10 cm. Goodman (1969) made several models of the Jovian

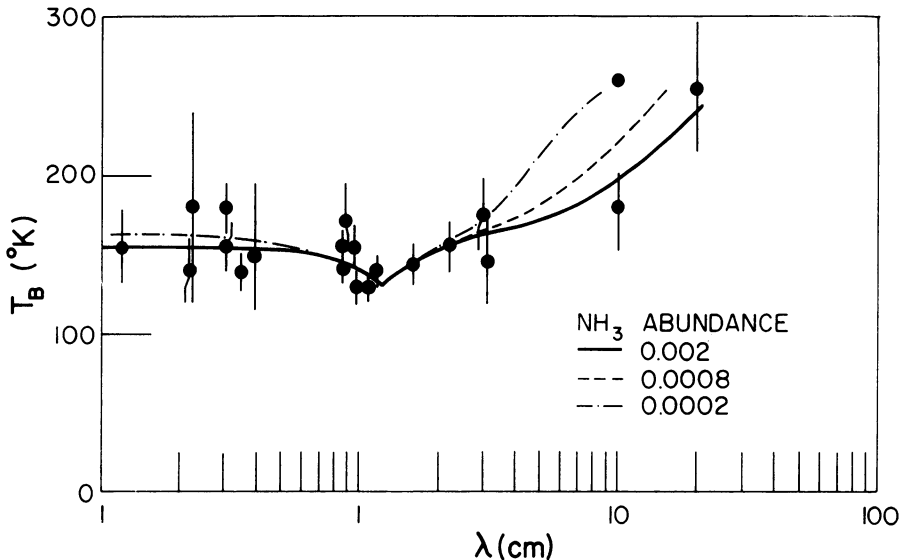


Fig. 8. Jovian thermal spectrum. The data points shown are from Dickel *et al.* (1970).

atmosphere without a cloud layer and according to his results we would have to raise the ammonia mixing ratio in the upper atmosphere to 0.002 in order to approach the current degree of flattening. Optical observational results (Goody, 1969; Owen, 1969) indicate values closer to 0.0008. Our spectrum, however, is in excellent agreement with models obtained by Hogan *et al.* (1969) where they used cloud-top temperatures near 200 K and an ammonia mixing ratio of 0.001. Sources below the top of the dense cloud layer were not considered in those models. Thus, it is possible that the cloud layer is opaque to microwave radiation because of strong scattering by water ice or other aerosols which may exist in the region or in the lower atmosphere.

4. Conclusion

In summary, the Stokes parameters of synchrotron emission were integrated over a given dipolar shell and obtained as function of surface magnetic field, electron energy and electron pitch angle distributions. The integration takes into account the partial eclipse of the dipolar shells by the planet at different System III longitudes. The solution consists of the belt characteristics which give the best match with the observational data, i.e., the interferometric and occultation data, the variability studies, and the spectral profiles of the intensity and of the degree of polarization. The results indicate a relatively flat non-thermal spectrum to frequencies even higher than 3000 MHz such that the thermal component of emission is less than previously expected.

Acknowledgements

This research was supported by the National Aeronautics and Space Administration Grant NGR 14-005-176.

References

- Berge, G. L.: 1966, *Astrophys. J.* **146**, 767.
Branson, N. J.-B. A.: 1968, *Monthly Notices Roy. Astron. Soc.* **139**, 155.
Dickel, J. R., Degioanni, J., and Goodman, G.: 1970, *Radio Sci.* **5**, 517.
Goodman, G.: 1969, *Models of Jupiter's Atmosphere*, Ph.D. Thesis, University of Illinois, Urbana.
Goody, R.: 1969, *J. Atmospheric Sci.* **24**, 997.
Gulkis, S.: 1970, *Radio Sci.* **5**, 505.
Hogan, J. S., Rasool, S. I., and Encrenaz, T.: 1969, *J. Atmospheric Sci.* **24**, 898.
Melrose, D. B.: 1967, *Planetary Space Sci.* **15**, 381.
Owen, T.: 1969, *Icarus* **10**, 355.
Roberts, J. A. and Ekers, R. D.: 1968, *Icarus* **8**, 160.